


Article

The Combined Partial Knockdown of *CBS* and *MPST* Genes Induces Inflammation, Impairs Adipocyte Function-Related Gene Expression and Disrupts Protein Persulfidation in Human Adipocytes

Jessica Latorre ^{1,2}, Angeles Aroca ³, José Manuel Fernández-Real ^{1,2,4}, Luis C. Romero ³
and José María Moreno-Navarrete ^{1,2,*}

- ¹ Department of Diabetes, Endocrinology and Nutrition, Institut d'Investigació Biomèdica de Girona (IdIBGi), 17190 Salt, Spain; jlatorre@idibgi.org (J.L.); jmfreal@idibgi.org (J.M.F.-R.)
² CIBER Fisiopatología de la Obesidad y Nutrición (CIBERObn, CB06/03/010), Instituto de Salud Carlos III, 28029 Madrid, Spain
³ Instituto de Bioquímica Vegetal y Fotosíntesis, Consejo Superior de Investigaciones and Universidad de Sevilla, 41092 Seville, Spain; aaroca@us.es (A.A.); lromero@ibvf.csic.es (L.C.R.)
⁴ Department of Medicine, Universitat de Girona, 17003 Girona, Spain
* Correspondence: jmoreno@idibgi.org; Tel.: +34-872-987087 (ext. 70)



Citation: Latorre, J.; Aroca, A.; Fernández-Real, J.M.; Romero, L.C.; Moreno-Navarrete, J.M. The Combined Partial Knockdown of *CBS* and *MPST* Genes Induces Inflammation, Impairs Adipocyte Function-Related Gene Expression and Disrupts Protein Persulfidation in Human Adipocytes. *Antioxidants* **2022**, *11*, 1095. <https://doi.org/10.3390/antiox11061095>

Academic Editors: Emma Mitidieri and Vincenzo Brancaleone

Received: 29 March 2022

Accepted: 27 May 2022

Published: 31 May 2022

Publisher's Note: MDPI stays neutral with regard to jurisdictional claims in published maps and institutional affiliations.



Copyright: © 2022 by the authors. Licensee MDPI, Basel, Switzerland. This article is an open access article distributed under the terms and conditions of the Creative Commons Attribution (CC BY) license (<https://creativecommons.org/licenses/by/4.0/>).

Abstract: Recent studies in mice and humans demonstrated the relevance of H₂S synthesising enzymes, such as CTH, CBS, and MPST, in the physiology of adipose tissue and the differentiation of preadipocyte into adipocytes. Here, our objective was to investigate the combined role of CTH, CBS, and MPST in the preservation of adipocyte protein persulfidation and adipogenesis. Combined partial *CTH*, *CBS*, and *MPST* gene knockdown was achieved treating fully human adipocytes with siRNAs against these transcripts (siRNA_MIX). Adipocyte protein persulfidation was analyzed using label-free quantitative mass spectrometry coupled with a dimedone-switch method for protein labeling and purification. Proteomic analysis quantified 216 proteins with statistically different levels of persulfidation in KD cells compared to control adipocytes. In fully differentiated adipocytes, *CBS* and *MPST* mRNA and protein levels were abundant, while *CTH* expression was very low. It is noteworthy that siRNA_MIX administration resulted in a significant decrease in *CBS* and *MPST* expression, without impacting on *CTH*. The combined partial knockdown of the *CBS* and *MPST* genes resulted in reduced cellular sulfide levels in parallel to decreased expression of relevant genes for adipocyte biology, including adipogenesis, mitochondrial biogenesis, and lipogenesis, but increased proinflammatory- and senescence-related genes. It should be noted that the combined partial knockdown of *CBS* and *MPST* genes also led to a significant disruption in the persulfidation pattern of the adipocyte proteins. Although among the less persulfidated proteins, we identified several relevant proteins for adipocyte adipogenesis and function, among the most persulfidated, key mediators of adipocyte inflammation and dysfunction as well as some proteins that might play a positive role in adipogenesis were found. In conclusion, the current study indicates that the combined partial elimination of *CBS* and *MPST* (but not *CTH*) in adipocytes affects the expression of genes related to the maintenance of adipocyte function and promotes inflammation, possibly by altering the pattern of protein persulfidation in these cells, suggesting that these enzymes were required for the functional maintenance of adipocytes.

Keywords: human adipocytes; adipogenesis; inflammation; protein persulfidation

1. Introduction

Functional adipocytes are characterized by an increased capacity to store excess fuel and produce beneficial adipokines, increased expression of adipogenic genes, but decreased expression of proinflammatory- and cellular senescence-related genes [1–4]. Optimal

adipocyte function is required to maintain adipose tissue physiology and prevents obesity-associated metabolic disturbances [3–6].

Recent studies in mice and humans demonstrated the relevance of H₂S-synthesising enzymes, such as CTH, CBS, and MPST, to preserve adipogenesis of adipose tissue, healthy fat mass expansion and insulin action [7,8]. These enzymes play a crucial role in the differentiation of adipocytes. Specifically, gene knockdown experiments in mouse 3T3-L1 cells and human preadipocytes demonstrated the relevance of CTH, CBS and MPST in adipogenesis [7–9]. Interestingly, increased persulfidation in relevant adipogenic proteins has also been reported in human adipocytes [8]. Since persulfidation often increases the reactivity of target proteins [10], increased persulfidation in adipogenic enzymes suggests a possible role of these post-translational modifications in the promotion of adipocyte differentiation and in the maintenance of adipogenic status. Despite these intriguing studies, to the best of our knowledge, the combined role of these enzymes in the maintenance of adipocyte function has not been yet examined.

In the present study, our objective was to investigate the combined role of CTH, CBS, and MPST in the preservation of adipocyte adipogenesis and function and to investigate how the combined partial knockdown of these enzymes might impact the persulfidation of the adipocyte proteins.

2. Materials and Methods

2.1. Human Preadipocyte Differentiation and Adipocyte Maintenance

Primary human subcutaneous preadipocytes from a non-diabetic Caucasian female with BMI < 30 kg/m² (Zen-Bio Inc., Research Triangle Park, Durham, NC, USA) were cultured with Preadipocyte Medium (PM-1, Zen-Bio Inc.) in a humidified incubator at 37 °C with 5% CO₂. Twenty-four hours after plating, cells were checked for confluence. Once reached, differentiation started with commercially available Differentiation Medium (DM-2, Zen-Bio Inc.) and Maintenance Medium (AM-1 Zen-Bio Inc.), following the manufacturer's instructions. Two weeks after initiating differentiation, differentiated cells appeared rounded with large lipid droplets apparent in the cytoplasm. The cells were then considered mature adipocytes. Forward siRNA transfections using siRNA_MIX, which included siRNAs against *MPST*, *CBS*, and *CTH* gene expression, were performed at the end of the differentiation process.

2.2. siRNA-Induced Gene Knockdown in Fully Differentiated Adipocytes

Primary human subcutaneous adipocytes were forward transfected with siRNAs at the end of differentiation (on day 11). Briefly, siRNA (Sigma-Aldrich, St. Louis, MO, USA) against CTH (NM_001190463), CBS (NM_000071), and MPST (NM_001130517) and Lipofectamine RNAiMAX (Life Technologies, Darmstadt, Germany) were diluted separately with Opti-MEM I Reduced Serum Medium (Life Technologies, Darmstadt, Germany) and mixed by pipetting afterwards. The siRNA-RNAiMAX complexes were left to incubate for 20 min at room temperature and then added to the top of the adherent cells drop-wise. The final concentrations of Lipofectamine RNAiMAX and siRNAs were 1.6 µL/cm² and 100 nM, respectively, in 12-well cell culture plates, and the final amount of medium per well was 1 mL. The transfection conditions included combined silencing of CTH, CBS and MPST (100 nM), and a non-targeting siRNA (100 nM) for the vehicle. Adipocytes were harvested on day 14 of differentiation, i.e., 72 h after transfection without changing cell culture medium. Transfection efficiency was assessed by real-time PCR and Western blot. The MISSION[®] siRNAs (Sigma-Aldrich) used were MISSION[®] esiRNA targeting human MPST (EHU086511), CBS (EHU099041), and CTH (EHU078251). The MISSION[®] siRNA Universal Negative Control #1 (Sigma-Aldrich, SIC001) was used as a control in all experiments (siRNA_SCR).

2.3. Gene Expression

RNA was extracted from cells using the RNeasy Lipid Tissue Mini Kit (Qiagen, Germantown, MD, USA). Total RNA was quantified using a spectrophotometer (GeneQuant; GE Health Care, Waukesha, WI, USA). RNA was reverse transcribed to cDNA using the High-Capacity cDNA Reverse Transcription Kit (Life Technology, Darmstadt, Germany) according to standard procedures. Commercially available Taq-Man primer and probe sets were used for gene expression. Expression was assessed by real-time PCR using the LightCycler 480 Real-Time PCR System (Roche Diagnostics, Barcelona, Spain).

The commercially available and pre-validated TaqMan[®] primer/probe sets used were as follows: Peptidylprolyl isomerase A (cyclophilin A) (4333763, *PPIA* as endogenous control), cystathionine γ -lyase (*CTH*, Hs00542284_m1), cystathionine β -synthase (*CBS*, Hs00163925_m1), mercaptopyruvate sulfurtransferase (*MPST*, Hs00560401_m1), adiponectin (*ADIPOQ*, Hs00605917_m1), fatty acid binding protein 4, adipocyte (*FABP4*, Hs01086177_m1), peroxisome proliferator-activated receptor gamma (*PPARG*, Hs00234592_m1), perilipin 1 (*PLIN1*, Hs00160173_m1), PPARG coactivator 1 alpha (*PPARGC1A*, Hs00173304_m1), fatty acid synthase (*FASN*, Hs00188012_m1), acetyl-CoA carboxylase alpha (*ACACA*, Hs00167385_m1), solute carrier family 2 member 4 (*SLC2A4* or *GLUT4*, Hs00168966_m1), interleukin 6 (interferon, beta 2) (*IL6*, Hs00985639_m1), tumor necrosis factor (*TNF*, Hs00174128_m1), C-X-C motif chemokine ligand 8 (*CXCL8* or *IL8*, Hs00174103_m1), C-C motif chemokine ligand 2 (*CCL2* or *MCP1*, Hs00234140_m1), and tumor protein p53 (*TP53*, Hs01034249_m1).

2.4. Western Blot

The proteins were extracted from cells using radioimmunoprecipitation assay (RIPA) buffer (0.1% SDS, 0.5% sodium deoxy-cholate, 1% Nonidet P-40, 150 mmol/L NaCl, and 50 mmol/L Tris-HCl, pH 8.0) supplemented with a commercially available cocktail of protease inhibitors (Millipore, Sigma, Madrid, Spain). Cellular debris and lipids were eliminated by centrifugation of the solubilized samples at $12,000 \times g$ for 10 min at 4 °C, recovering the soluble fraction. The protein concentration was determined using the RC/DC Protein Assay (Bio-Rad Laboratories, Hercules, CA, USA). Protein extracts were processed in SDS-PAGE and transferred to nitrocellulose membranes by conventional procedures. After blocking with 5% BSA in TBS-Tween, the membranes were incubated with primary antibodies, followed by incubation with horseradish peroxidase conjugated goat anti-rabbit antibody (Cell Signaling, 7074). Protein signal was detected by chemiluminescence Chemi-Doc[™] Gel Imaging System (Bio-Rad, California, USA). Actin was used as a housekeeping gene-coded protein. All primary antibodies were used at 1:1000 dilutions and were the following: CBS (sc-133154, Santa Cruz Biotechnology, Santa Cruz, CA, USA), CTH (sc-365382, Santa Cruz Biotechnology), MPST (sc-376168, Santa Cruz Biotechnology), FAS (C20G5, Cell Signaling), and β -actin (sc-47778, Santa Cruz Biotechnology).

2.5. Quantification of Hydrogen Sulfide in Biological Matrices by LC-MS/MS

Hydrogen sulfide was quantified following a previously described method [11]. A 50 μ L sample (cell lysate) was spiked with 70 μ L of MBB solution (20 mM). The mixture was vortexed, incubated for 60 min at room temperature, and the derivatization reaction stopped by adding 10 μ L 20% formic acid. The mixture was subjected to centrifugation at $12,000 \times rpm$ for 10 min. The derivative sulfide dibimane was analyzed by LC-MS/MS using the ExionLC[™] UPLC system (Sciex, Framingham, MA, USA) with a reversed-phase column (100 mm \times 4.6 mm \times 100 \AA particle, Kinetex XB-C18, Phenomenex, Torrance, CA, USA). The mobile phases were 0.1% formic acid in H₂O (Buffer A, HPLC/LCMS grade) and 0.1% formic acid in acetonitrile (Buffer B, HPLC/LC-MS grade). A 5 μ L sample was loaded per injection, and the gradient, applied at a flow rate of 600 μ L min⁻¹, was as follows: 1.7 min 80% A, from 1.7 to 3 min linear gradient from 80% A to 20% A, 1 min isocratic 20% A, 1 min linear gradient from 20% A to 80% A, and hold 3 min at 80% A to re-equilibrate the column. Mass spectra were acquired using a QTRAP 6500 + triple quadrupole (Sciex, Framingham, MA, USA) equipped with an electrospray ionization source operating in

negative ionization mode using an ion spray voltage of -4500 V. The other ESI parameters were as follows: curtain gas, 35 psi; collision gas, medium; temperature, 500 °C; nebulizer gas (GS1), 60 psi; and heater gas (GS2), 60 psi. Data were acquired with Analyst[®] 1.7 software in the multiple reaction monitoring (MRM) mode with a detection window of 60 s. The measured ionization adducts $[M-H]^-$ selected for identification and quantification were 412.9 m/z (Q1) and 190.9 m/z (Q3) and optimized declustering potential (DP – 45 V) and collision energy (CE – 24 V). Data were processed with Sciex OS[®] software (Sciex, Redwood City, CA, USA) for peak integration and quantification.

2.6. Protein Persulfidation

A total of 500 µg of proteins from adipocyte lysates in 50 mM Tris-HCl, pH 8, supplemented with 1% protease inhibitor (cOmplete[™], SigmaAldrich) and 2% SDS was incubated with 5 mM 4-chloro-7-nitrobenzofurazan (Cl-NBF) at 37 °C for 30 min, protected from light. A methanol/chloroform precipitation was performed to eliminate excess Cl-NBF, and protein pellets obtained were washed with cold methanol, dried, and dissolved in 50 mM Tris-HCl, pH 8, with 2% SDS, as previously described [12,13]. The proteins were then incubated with 100 µM DCP-Bio1 at 37 °C for 1.5 h. Afterwards, proteins were precipitated with methanol/chloroform and dissolved in 50 mM Tris-HCl, pH 8, supplemented with 0.1% SDS. Proteins were incubated with Sera-Mag[™] Magnetic Streptavidin (Cytiva, Madrid, Spain) at 4 °C overnight with agitation and then, beads were washed with 8 column volumes of 50 mM Tris-HCl, pH 8, with 0.001% Tween, 2 column volumes of 50 mM Tris-HCl, pH 8, and 1 column volume of pure HPLC-quality water. After washing, beads were incubated 5 h with agitation with 2.25 M ammonium hydroxide at RT. The sample was then neutralized with formic acid and the protein concentration was determined. A total of 50 µg of proteins were trypsinized (GOLD, Promega) following the filter-aided sample preparation (FASP) method [14]. Trypsin was added to a trypsin:protein ratio of 1:20, and the mixture was incubated overnight at 37 °C, dried out in a RVC2 25 speedvac concentrator (Christ), and resuspended in 0.1% FA. Peptides were desalted and resuspended in 0.1% FA using C18 stage tips (Millipore). The samples were analyzed in a timsTOF Pro with PASEF (Bruker Daltonics, Billerica, MA, USA) coupled online to an Evosep ONE liquid chromatograph (Evosep). Hence, 200 ng were directly loaded onto the Evosep ONE and resolved using the 30 samples-per-day protocol. The processed data were analyzed with the MQ (Max Quant) search engine and the label-free quantification was performed using PEAKS Studio (BSI, Mississauga, Canada) [15]. Protein identification and quantification were carried out using PEAKS X software (Bioinformatics solutions). The searches were carried out against a database consisting of *Homo sapiens* (Uniprot/Swissprot), with precursor and fragment tolerances of 20 ppm and 0.05 Da. Only proteins identified with at least two peptides at FDR < 1% were considered for further analysis. Protein abundances inferred from PEAKS were loaded onto Perseus computational platform [16], log₂ transformed, and imputed. A *t*-test was used to address significant differences in protein abundances within each sample group under analysis.

The mass spectrometry proteomics data have been deposited in the ProteomeXchange Consortium [17] via the PRIDE partner repository with the dataset identifier PXD032370 and 10.6019/PXD032370.

Functional protein association networks were explored using the STRING database (STRING: functional protein association networks (string-db.org) access date 26 February 2022).

2.7. Statistical Analysis

Statistical analyses were performed using SPSS 12.0 software. The unpaired *t*-test and nonparametric test (Mann–Whitney test) were used to analyze in vitro experimental data. The levels of statistical significance were set at $p < 0.05$.

3. Results and Discussion

3.1. The Relevance of CTH, CBS and MPST on Human Adipocytes

In fully differentiated adipocytes, *CBS* and *MPST* mRNA and protein levels were abundant, whereas *CTH* expression was very low (Figure 1A,B). It should be noted that siRNA_MIX administration resulted in a significant decrease in *CBS* and *MPST* expression, without impacting on *CTH* (Figure 1A,B). Possibly, the very low transcription and turnover of *CTH* make it resistant to the effect of siRNA. The combined partial knockdown of *CBS* and *MPST* genes led to a significant reduction in cellular sulfide levels (Figure 1C), indicating that H₂S biosynthesis was attenuated in these cells. Interestingly, the combined partial *CBS* and *MPST* gene knockdown also resulted in decreased expression of relevant genes for adipocyte biology, including adipogenesis (*ADIPOQ*, *FABP4*, *PLIN1*, *SLC2A4*, *PPARG*), mitochondrial biogenesis (*PPARGC1A*), and lipogenesis (*ACACA* and *FASN* mRNA, and *FAS* protein) (Figure 1D–L), but increased proinflammatory- and senescence-related genes (*TP53*) (Figure 1M–Q). Importantly, these data indicated that *MPST* and *CBS* were not only required during adipocyte differentiation of mouse 3T3-L1 cells [9] or human preadipocytes [8], but these proteins were also necessary for the functional maintenance of adipocytes. In contrast to that observed during adipocyte differentiation or in mouse 3T3-L1 adipocytes [7,18,19], in fully differentiated human adipocytes, the expression of *CTH* was much lower than *CBS* and *MPST*.

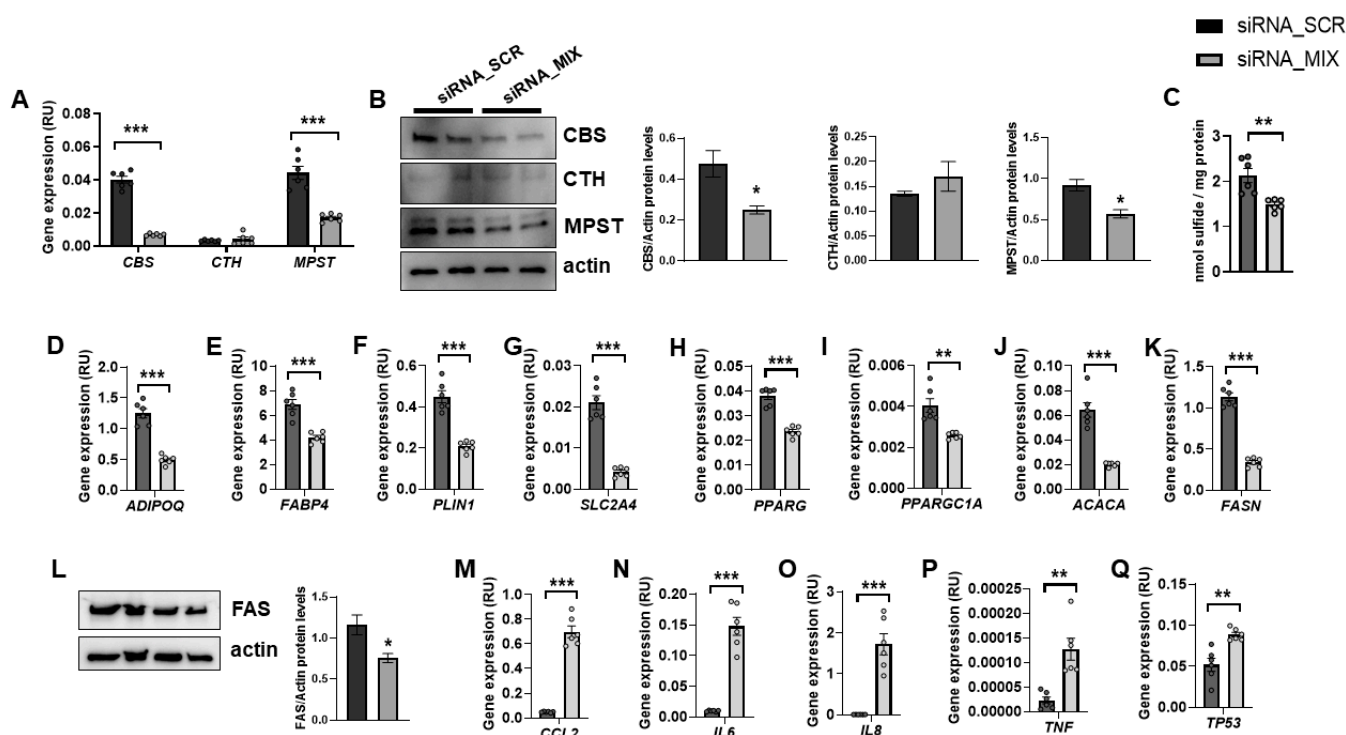


Figure 1. The impact of the combined partial knockdown of *CBS* and *MPST* gene on relevant genes for adipocyte biology. The effect of siRNA_MIX administration on *CBS*, *CTH* and *MPST* mRNA (A) and protein (B) levels, on intracellular sulfide levels (C), and on expression of adipogenic (*ADIPOQ*, *FABP4*, *PLIN1*, *SLC2A4*, *PPARG*, *PPARGC1A*)-, lipogenic (*ACACA*, *FASN*)-, proinflammatory (*CCL2*, *IL6*, *IL8*, *TNF*)- and cellular senescence (*TP53*)-related genes and on *FAS* protein levels (D–Q). * $p < 0.05$, ** $p < 0.01$ and *** $p < 0.001$ compared to siRNA_SCR.

No visual differences in lipid droplets were observed between control and combined partial knockdown cells (data not shown). Considering that adipocyte dedifferentiation becomes morphologically evident at least one week after the start of the process [20], longer gene knockdown experiments should be required to appreciate significant changes in intracellular lipid accumulation.

3.2. Impact of the Combined Partial Knockdown of MPST and CBS Genes on Adipocyte Protein Persulfidation

The possible link between CTH, CBS, and MPST activities and protein persulfidation during human adipocyte differentiation [8] suggests that these enzymes might modulate persulfidation in several adipogenic proteins, affecting the physiology of adipocytes. To test this hypothesis, we examined whether the reduction of adipogenic markers observed in human adipocytes with the combined partial knockdown of *MPST* and *CBS* genes was linked to altered persulfidation in key adipogenic proteins. For this purpose, we used a mass spectrometry label-free quantitative proteomic approach combined with the dimedone-switch method to measure the protein profile of persulfidation. Proteins from three biological replicates from fully differentiated human adipocytes, control, and the combined partial *MPST* and *CBS* gene knockdown were isolated and subjected to the dimedone-switch procedure for isolation of the persulfidated proteins. The proteomic analysis quantified 1834 proteins with a FDR threshold of 1% (Supplementary Dataset S1) of which 216 showed statistically different levels of persulfidation in KD cells compared to control adipocytes (Student *t*-test, $p < 0.05$) (Supplementary Dataset S2). From these proteins, 136 proteins were less persulfidated in KD cells, and 80 proteins were more persulfidated.

When functional protein association networks were explored using the STRING database, we found that those differentially less persulfidated proteins in human adipocytes with the combined partial knockdown of *MPST* and *CBS* genes were associated with relevant metabolic processes for adipocytes. These processes included the biosynthetic process of acetyl-CoA and acyl-CoA, tricarboxylic acid cycle, the metabolic process of pyruvate and glucose, extracellular matrix organization, the regulation of the mRNA stability, metabolic process of sulfur compound, the oxidation-reduction process, and the regulation of catabolic process (FDR < 0.02, Figure 2A). Otherwise, differentially increased persulfidated proteins in human adipocytes with the combined partial knockdown of *MPST* and *CBS* genes were mainly associated with processes related to immune response- and cytokine-mediated signaling pathways (FDR < 0.005, Figure 2B).

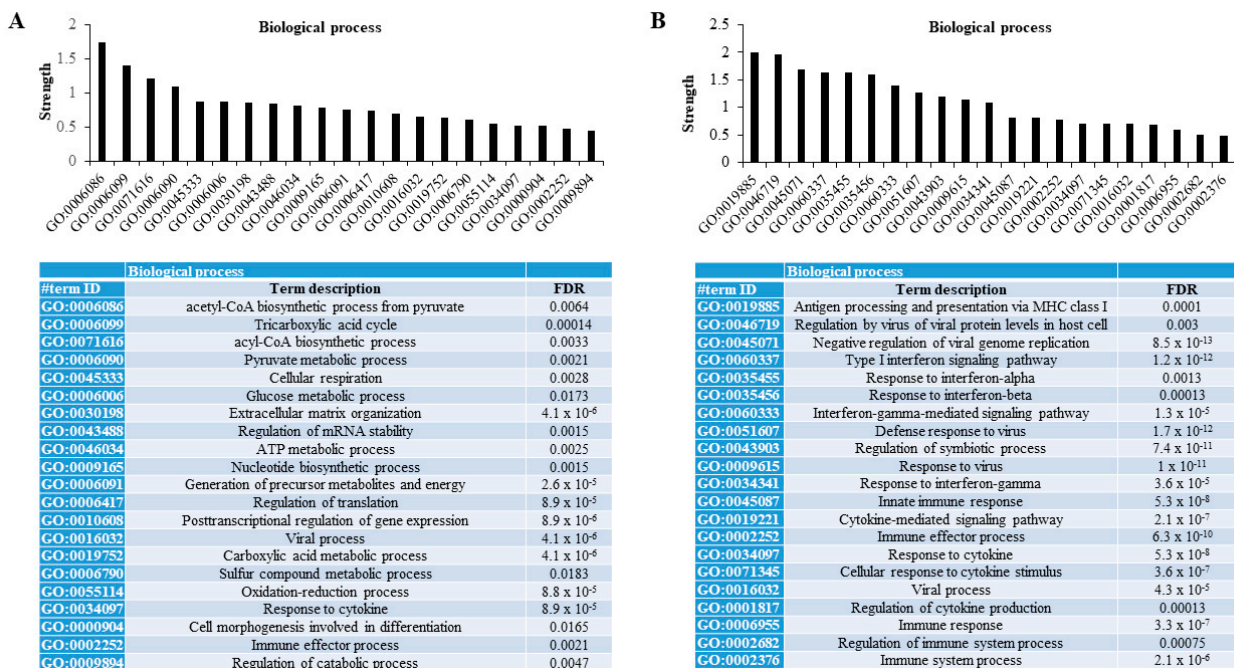


Figure 2. Proteomic persulfidation networks analysis. Analysis of functional protein association networks using STRING database of differentially decreased (A) and increased (B) persulfidated proteins in siRNA_MIX- compared to siRNA_SCR-treated cells. FDR, false discovery rate adjusted *p*-value.

Specifically, among those proteins found less persulfidated, several relevant proteins for the maintenance of adipocyte adipogenesis and function were identified, including RAB4A, IDH2, ITGA5, NPC1, ACO1, LRP1, AHNAK, ARPC3, ADH1B, ALDH1A3, LGALS1, PHB, COL6A3, PLIN3, FABP4, THBS1, ANXA2, PLIN4, ACSL1, ANXA1, ELAVL1, ALDH1A1, and HNRNPA1 (Figure 3A, all with $p < 0.05$). Previous studies supported the relevance of these proteins in adipocyte biology. RAB4A is a small GTPase that participates in adipocyte GLUT4 trafficking, exerting an important role in glucose uptake [21,22]. IDH2 attenuates adipocyte inflammation through the induction of α -ketoglutarate production [23] and is required for lipogenesis in these cells [24]. ITGA5 promotes fibrosis of adipose tissue [25] and inhibits adipocyte differentiation in human adipose tissue-derived stem cells [26]. Decreased expression of the NPC1 gene or the partial deletion of this gene promoted weight gain and fat mass expansion [27–29], suggesting a relevant role of NPC1 in the prevention of obesity and adipocyte hypertrophy, possibly increasing lipolysis and beta oxidation and decreasing lipogenesis and triglyceride accumulation in adipocytes [30]. NPC1 is increased in adipocytes [31], but it was not associated with adipogenesis [32]. ACO1 is important to maintain adipogenesis in adipocytes, possibly modulating cytosolic NADPH levels and intracellular iron homeostasis, both processes required for adipocyte biology [33]. LRP1 is required for adipocyte differentiation and to maintain adipocyte adipogenesis [34], possibly in part due to its interaction with ShcA [35], or acting as APOA4 receptor, and favoring APOA4-induced glucose uptake [36]. Several studies have demonstrated that AHNAK is required for adipocyte differentiation [37–39]. Mechanistically, a recent study demonstrated that AHNAK gene knockdown decreased adipogenesis through the suppression of Bmpr1 α expression and decreased BMP4/ Bmpr1 α signaling [39]. ARPC3 is another protein required for adipocyte differentiation, exerting a relevant role in the late stage of the process, participating in GLUT4 exocytosis and insulin signal transduction, and suggesting a relevant role in maintaining insulin action in adipocytes [40]. ADH1B modulates intracellular lipid accumulation, without impacting adipogenesis [41], and preserved insulin-stimulated glucose uptake in adipocytes [42]. Inhibition of ALDH1A1 reduced visceral fat [43], negatively impacting adipogenesis in visceral adipose tissue [44]. LGALS1 (galectin 1) is an adipocyte secreted factor [45] that enhances the transcriptional activity of PPAR γ , increasing adipogenesis and accumulation of lipids in adipocytes [46]. Gain–loss in vivo studies demonstrated that this protein is crucial for adipose tissue expansion and adiposity [46]. LGALS1 expression in subcutaneous adipose tissue has been identified as a relevant factor to confer the risk of weight regain [47]. Pharmacological inhibition of LGALS1 displayed important anti-obesogenic and anti-adipogenic effects [48,49], strengthening the role of this protein in the development of fat mass and obesity. Otherwise, circulating galectin-1 levels were negatively associated with type 2 diabetes [50,51], indicating that it might be associated with healthy adiposity. PHB is induced during adipocyte differentiation, in response to insulin and PPAR γ agonist, and its overexpression in 3T3-L1 fibroblasts was sufficient to induce adipogenesis [52], but its gene knockdown reduces the expression of adipogenic genes and lipid accumulation and impairs mitochondrial dysfunction [53,54]. In adipocytes, prohibitin is required for fatty acid uptake [55]. COL6A3 gene knockdown increased the triglyceride content, lipolysis, insulin-induced Akt phosphorylation, and the expression of adipogenic genes (peroxisome proliferator-activated receptor- γ , glucose transporter, adiponectin, and fatty acid binding protein), indicating improved adipocyte function and insulin sensitivity [56]. In addition, COL6A3 knockdown also decreased basal adipocyte MCP1 mRNA expression, reduced secreted protein levels, and attenuated TNF α - and LPS-induced MCP1 gene expression [57]. In contrast, increased COL6A3 mRNA in adipocytes is associated with obesity, insulin resistance, and inflammation of adipose tissue [58,59], supporting the negative impact of this protein on adipocytes and adipose tissue. Annexin A1 (AnxA1) is an endogenous glucocorticoid regulated protein that modulates systemic anti-inflammatory processes. AnxA1 gene expression and protein were significantly up-regulated during adipogenesis in human SGBS preadipocytes [60]. Epididymal fat mass was reduced by ANXA1 gene

deletion, but adipocyte size was unchanged, suggesting that ANXA1 is required for maintaining adipocyte cell number [61]. Furthermore, the progressive accumulation of Annexin A2 (AnxA2) in the myofiber matrix causes muscle-resident fibro/adipogenic precursors (FAP) differentiation into adipocytes, and depletion of AnxA2 prevents FAP adipogenesis and muscle loss [62]. ACSL1 is required for beta oxidation in adipocytes, and it is associated to adipose insulin sensitivity, adipogenesis and adipocyte fatty acid uptake [63–70]. ELAVL1 (also named HuR) is an important repressor of adipogenesis. Knockdown and overexpression of HuR in primary adipocyte culture enhances and inhibits adipogenesis, respectively [71]. HuR also exerts an important role in the prevention of adipocyte hypertrophy and inflammation of adipose tissue [72]. However, previous studies in 3T3-L1 cells indicate that HuR is required in early events of adipogenesis, allowing C/EBP β mRNA translocation into the cytosol, and its proper translation, a process required to activate CEBP α and PPAR γ in mitotic clonal expansion [73,74]. Importantly, the reduction in HuR persulfidation, resulted in the stabilization of HuR-target mRNAs, and increased its translation and expression [75], suggesting that the decrease in HuR persulfidation improved HuR dimerization and its activity, and consequently, it has negative effects on adipocyte adipogenesis. Interestingly, perilipin persulfidation inhibits lipid mobilization and lipolysis in adipocytes, and contributes to adequate maintenance of lipid storage [76]. HNRNPA1 is a known regulator of INSR exon 11 splicing, which could have an impact on adipose insulin action [77].

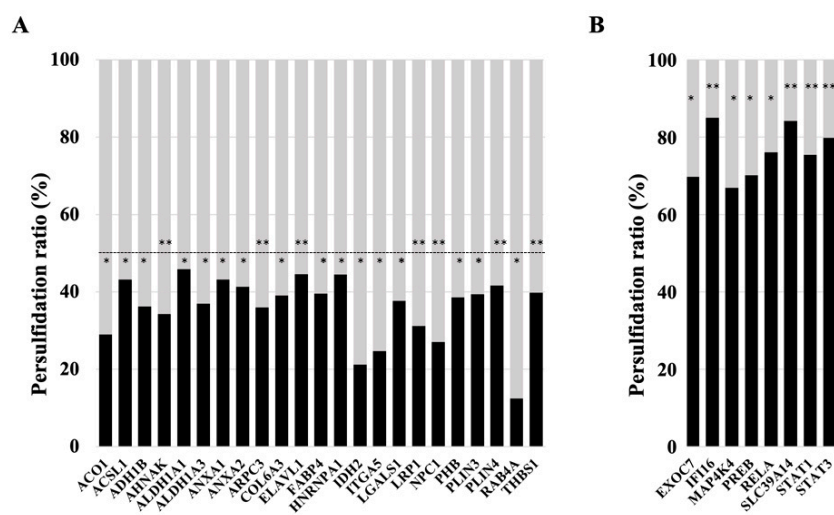


Figure 3. Rate of persulfidation of relevant proteins involved in adipocyte function and the maintenance of adipogenesis. Level of protein persulfidation in siRNA_MIX samples (black boxes, in percentage) compare to the level in control samples (grey boxes). (A) ACO1, Cytoplasmic aconitate hydratase; ACSL1, Long-chain-fatty-acid—CoA ligase 1; ADH1B, All-trans-retinol dehydrogenase [NAD(+)] ADH1B; AHNAK, Neuroblast differentiation-associated protein AHNAK; ALDH1A1, Retinal dehydrogenase 1; ALDH1A3, Aldehyde dehydrogenase family 1 member A3; ANXA1, Annexin A1; ANXA2, Annexin A2; ARPC3, Actin-related protein 2/3 complex subunit 3; COL6A3, Collagen alpha-3(VI) chain; ELAVL1, ELAV-like protein 1; FABP4, Fatty acid-binding protein adipocyte; HNRNPA1, Heterogeneous nuclear ribonucleoprotein A1; IDH2, Isocitrate dehydrogenase [NADP] mitochondrial; ITGA5, Integrin alpha-5; LGALS1, Galectin-1; LRP1, Low-density lipoprotein receptor-related protein 1; NPC1, NPC intracellular cholesterol transporter 1; PHB, Prohibitin; PLIN3, Perilipin-3; PLIN4, Perilipin-4; RAB4A, Ras-related protein Rab-4A; THBS1, Thrombospondin-1. (B) EXOC7, Exocyst complex component 7; IFI16, Gamma-interferon-inducible protein 16; MAP4K4, Mitogen-activated protein kinase kinase kinase kinase 4; PREB, Prolactin regulatory element-binding protein; RELA, Transcription factor p65; SLC39A14, Metal cation symporter ZIP14; STAT1, Signal transducer and activator of transcription 1-alpha/beta; STAT3, Signal transducer and activator of transcription 3. Student *t*-test significance: * $p < 0.05$; ** $p < 0.01$.

Among the most persulfidated proteins, some key mediators of adipocyte inflammation and dysfunction (IFI16, STAT3, RELA, STAT1, MAP4K4, PREB) were found, but also proteins that might have a positive role in adipogenesis (EXOC7, SLC39A14) (Figure 3B, all with $p < 0.05$). In mice and humans, increased IFI16 levels are associated with larger adipocytes, enhanced inflammatory state, and impaired insulin-stimulated glucose uptake in white adipose tissue [78]. STAT3 is a relevant transcription factor of proinflammatory genes in adipocytes that is associated with adipocyte inflammation [79,80]. RELA is a relevant transcription factor associated with adipocyte inflammation [81] that inhibits adipogenesis and accumulation of lipids in adipocytes [82]. The activation of STAT1 transcription factor inhibits adipogenesis and promotes adipocyte and adipose tissue inflammation [83–88]. Isolated mature adipocytes from obese individuals had increased expression of mitogen-activated protein 4 kinase 4 (MAP4K4), which is known to inhibit PPAR γ transcriptional activity, adipogenesis, and insulin-stimulated glucose transport [89,90]. In line with this, MAP4K4 inhibits adipose lipogenesis via the suppression of Srebp-1 [91], and deletion of this kinase increases insulin sensitivity in adipose tissue [92]. Prolactin regulatory element-binding (PREB) is a negative regulator of adiponectin gene expression in adipocytes [93].

On the other hand, EXOC7 might participate in Glut4 trafficking [94,95], and SLC39A14 is a zinc transporter, which is rapidly induced in the early stages of differentiation, suggesting a possible role in adipogenesis [96]. In fact, depletion of SLC39A14 caused hypertrophy and inflammation of adipocytes [97].

These data indicated that the combined partial knockdown of the MPST and CBS genes disrupts the pattern of protein persulfidation in human adipocytes, suggesting a possible link between this disruption and adipocyte dysfunction, which is characterized by decreased adipogenesis but increased inflammation. This disruption included a significant decrease in persulfidation in key proteins for adipocyte function (RAB4A, IDH2, NPC1, ACO1, LRP1, AHNAK, ARPC3, ADH1B, ALDH1A1, LGALS1, PHB, ANXA1, ANXA2, ACSL1, PLIN3, PLIN4, FABP4, HNRNPA1), but also in proteins that negatively impact adipocytes and adipogenesis (ITGA5, COL6A3, ELAVL1). In addition, the combined partial knockdown of MPST and CBS genes in adipocytes resulted in increased persulfidation in relevant proinflammatory transcription factors (RELA, STAT1, STAT3) and anti-adipogenic proteins (IFI16, MAP4K4, PREB), but also in some proteins that might exert positive effects on adipogenesis, such as SLC39A14 and EXOC7. Persulfidation increases the reactivity of target proteins, modulating their biological activities [10]. However, it is important to note that modulation in persulfidation-induced protein activity can trigger activation or inhibition of the biological function of the persulfidated protein [98]. Other consequences of CBS and MPST gene knockdown, such as decreased H₂S biosynthesis [8,18] or increased homocysteine levels [99], could also explain the negative impact on adipocyte function. Additional experiments using specific chemical inhibitors of H₂S biosynthesis and the administration of H₂S donor molecules to CBS/MPST gene knockdown cells should be performed to further investigate the possible role of H₂S in this model.

Selenium-binding protein 1 (SELENBP1), a fourth enzyme that participates in H₂S biosynthesis, increased during differentiation of 3T3L1 adipocyte in association with lipogenesis and lipid accumulation, and it has been recently described as a marker of differentiated adipocytes [100]. SELENBP1 gene knockdown had a negative impact on adipocyte function in parallel to the decreased expression of the CBS, CTH, and MPST enzymes [101]. The contribution of other enzymes, such as SELENBP1 [100,101], or non-enzymatic pathways [102] in H₂S production cannot be excluded in the current study.

4. Conclusions

In summary, these findings indicate that the combined partial knockdown of CBS and MPST (but not CTH) in adipocytes impairs the expression of genes related with the maintenance of adipocyte function and promotes inflammation, possibly by disrupting the pattern of protein persulfidation in these cells. The current study points to the fact that

these enzymes were not only required during adipocyte differentiation [8,9], but they were also needed for the functional maintenance of adipocytes.

Supplementary Materials: The following supporting information can be downloaded at: <https://www.mdpi.com/article/10.3390/antiox11061095/s1>, Supplementary Dataset S1 and Supplementary Dataset S2.

Author Contributions: J.L. participated in this study conducting experiments, acquiring and analyzing data and reviewed the manuscript. A.A. and L.C.R. participated in this study acquiring and analyzing data, contributed to the discussion and reviewed the manuscript. J.M.F.-R. contributed to the discussion and reviewed the manuscript. J.M.M.-N. contributed to research study design, conducting experiments, acquiring and analyzing data, and writing the manuscript. All authors have read and agreed to the published version of the manuscript.

Funding: This work was partially supported by research grants PI16/01173, PI19/01712 and PI21/01361 from the Instituto de Salud Carlos III from Spain, Fondo Europeo de Desarrollo Regional (FEDER) funds, and VII Spanish Diabetes Association grants to Basic Diabetes Research Projects led by young researchers. This work was also partially supported by ERDF A way of making Europe, Junta de Andalucía (grant No. US-1255781).

Institutional Review Board Statement: Not applicable.

Informed Consent Statement: Not applicable.

Data Availability Statement: Data are available via ProteomeXchange with identifier PXD032370.

Acknowledgments: CIBEROBN Fisiopatología de la Obesidad y Nutrición is an initiative from the Instituto de Salud Carlos III from Spain.

Conflicts of Interest: The authors declared no conflict of interest.

References

1. Maurizi, G.; Della Guardia, L.; Maurizi, A.; Poloni, A. Adipocytes properties and crosstalk with immune system in obesity-related inflammation. *J. Cell. Physiol.* **2018**, *233*, 88–97. [[CrossRef](#)] [[PubMed](#)]
2. Sakers, A.; De Siqueira, M.K.; Seale, P.; Villanueva, C.J. Adipose-tissue plasticity in health and disease. *Cell* **2022**, *185*, 419–446. [[CrossRef](#)] [[PubMed](#)]
3. Virtue, S.; Vidal-Puig, A. Adipose tissue expandability, lipotoxicity and the Metabolic Syndrome—an allostatic perspective. *Biochim. Biophys. Acta* **2010**, *1801*, 338–349. [[CrossRef](#)] [[PubMed](#)]
4. Kim, J.Y.; Van De Wall, E.; Laplante, M.; Azzara, A.; Trujillo, M.E.; Hofmann, S.M.; Schraw, T.; Durand, J.L.; Li, H.; Li, G.; et al. Obesity-associated improvements in metabolic profile through expansion of adipose tissue. *J. Clin. Investig.* **2007**, *117*, 2621–2637. [[CrossRef](#)] [[PubMed](#)]
5. Vishvanath, L.; Gupta, R.K. Contribution of adipogenesis to healthy adipose tissue expansion in obesity. *J. Clin. Investig.* **2019**, *129*, 4022–4031. [[CrossRef](#)]
6. De Ferranti, S.; Mozaffarian, D. The perfect storm: Obesity, adipocyte dysfunction, and metabolic consequences. *Clin. Chem.* **2008**, *54*, 945–955. [[CrossRef](#)]
7. Yang, G.; Ju, Y.; Fu, M.; Zhang, Y.; Pei, Y.; Racine, M.; Baath, S.; Merritt, T.J.S.; Wang, R.; Wu, L. Cystathionine gamma-lyase/hydrogen sulfide system is essential for adipogenesis and fat mass accumulation in mice. *Biochim. Biophys. Acta Mol. Cell Biol. Lipids* **2018**, *1863*, 165–176. [[CrossRef](#)]
8. Comas, F.; Latorre, J.; Ortega, F.; Arnoriaga Rodríguez, M.; Kern, M.; Lluch, A.; Ricart, W.; Blüher, M.; Gotor, C.; Romero, L.C.; et al. Activation of Endogenous H(2)S Biosynthesis or Supplementation with Exogenous H(2)S Enhances Adipose Tissue Adipogenesis and Preserves Adipocyte Physiology in Humans. *Antioxid. Redox Signal.* **2021**, *35*, 319–340. [[CrossRef](#)]
9. Tsai, C.-Y.; Peh, M.T.; Feng, W.; Dymock, B.W.; Moore, P.K. Hydrogen sulfide promotes adipogenesis in 3T3L1 cells. *PLoS ONE* **2015**, *10*, e0119511. [[CrossRef](#)]
10. Filipovic, M.R. Persulfidation (S-sulfhydration) and H2S. *Handb. Exp. Pharmacol.* **2015**, *230*, 29–59. [[CrossRef](#)]
11. Tan, B.; Jin, S.; Sun, J.; Gu, Z.; Sun, X.; Zhu, Y.; Huo, K.; Cao, Z.; Yang, P.; Xin, X.; et al. New method for quantification of gasotransmitter hydrogen sulfide in biological matrices by LC-MS/MS. *Sci. Rep.* **2017**, *7*, 46278. [[CrossRef](#)] [[PubMed](#)]
12. Aroca, A.; Yruela, I.; Gotor, C.; Bassham, D.C. Persulfidation of ATG18a regulates autophagy under ER stress in Arabidopsis. *Proc. Natl. Acad. Sci. USA* **2021**, *118*, e2023604118. [[CrossRef](#)] [[PubMed](#)]
13. Zivanovic, J.; Kouroussis, E.; Kohl, J.B.; Adhikari, B.; Bursac, B.; Schott-Roux, S.; Petrovic, D.; Miljkovic, J.L.; Thomas-Lopez, D.; Jung, Y.; et al. Selective Persulfide Detection Reveals Evolutionarily Conserved Antiaging Effects of S-Sulfhydration. *Cell Metab.* **2019**, *30*, 1152–1170.e13. [[CrossRef](#)] [[PubMed](#)]

14. Wiśniewski, J.R.; Zougman, A.; Nagaraj, N.; Mann, M. Universal sample preparation method for proteome analysis. *Nat. Methods* **2009**, *6*, 359–362. [[CrossRef](#)] [[PubMed](#)]
15. Zhang, J.; Xin, L.; Shan, B.; Chen, W.; Xie, M.; Yuen, D.; Zhang, W.; Zhang, Z.; Lajoie, G.A.; Ma, B. PEAKS DB: De novo sequencing assisted database search for sensitive and accurate peptide identification. *Mol. Cell. Proteomics* **2012**, *11*, M111.010587. [[CrossRef](#)]
16. Tyanova, S.; Temu, T.; Sinitcyn, P.; Carlson, A.; Hein, M.Y.; Geiger, T.; Mann, M.; Cox, J. The Perseus computational platform for comprehensive analysis of (prote)omics data. *Nat. Methods* **2016**, *13*, 731–740. [[CrossRef](#)]
17. Vizcaíno, J.A.; Deutsch, E.W.; Wang, R.; Csordas, A.; Reisinger, F.; Ríos, D.; Dianes, J.A.; Sun, Z.; Farrah, T.; Bandeira, N.; et al. ProteomeXchange provides globally coordinated proteomics data submission and dissemination. *Nat. Biotechnol.* **2014**, *32*, 223–226. [[CrossRef](#)]
18. Cai, J.; Shi, X.; Wang, H.; Fan, J.; Feng, Y.; Lin, X.; Yang, J.; Cui, Q.; Tang, C.; Xu, G.; et al. Cystathionine γ lyase-hydrogen sulfide increases peroxisome proliferator-activated receptor γ activity by sulfhydration at C139 site thereby promoting glucose uptake and lipid storage in adipocytes. *Biochim. Biophys. Acta* **2016**, *1861*, 419–429. [[CrossRef](#)]
19. Comas, F.; Latorre, J.; Cussó, O.; Ortega, F.; Lluch, A.; Sabater, M.; Castells-Nobau, A.; Ricart, W.; Ribas, X.; Costas, M.; et al. Hydrogen sulfide impacts on inflammation-induced adipocyte dysfunction. *Food Chem. Toxicol. Int. J. Publ. Br. Ind. Biol. Res. Assoc.* **2019**, *131*, 110543. [[CrossRef](#)]
20. Sugihara, H.; Yonemitsu, N.; Miyabara, S.; Yun, K. Primary cultures of unilocular fat cells: Characteristics of growth in vitro and changes in differentiation properties. *Differentiation* **1986**, *31*, 42–49. [[CrossRef](#)]
21. Kaddai, V.; Gonzalez, T.; Keslair, F.; Grémeaux, T.; Bonnafous, S.; Gugenheim, J.; Tran, A.; Gual, P.; Le Marchand-Brustel, Y.; Cormont, M. Rab4b is a small GTPase involved in the control of the glucose transporter GLUT4 localization in adipocyte. *PLoS ONE* **2009**, *4*, e5257. [[CrossRef](#)] [[PubMed](#)]
22. Błaszczuk, M.; Gajewska, M.; Milewska, M.; Grzelkowska-Kowalczyk, K. Insulin-dependent cytoplasmic distribution of Rab4a in mouse adipocytes is inhibited by interleukin-6, -8, and -15. *Cell Biol. Int.* **2017**, *41*, 457–463. [[CrossRef](#)] [[PubMed](#)]
23. Liu, Z.; Gan, L.; Zhang, T.; Ren, Q.; Sun, C. Melatonin alleviates adipose inflammation through elevating α -ketoglutarate and diverting adipose-derived exosomes to macrophages in mice. *J. Pineal Res.* **2018**, *64*, e12455. [[CrossRef](#)] [[PubMed](#)]
24. Lee, S.J.; Kim, S.H.; Park, K.M.; Lee, J.H.; Park, J.-W. Increased obesity resistance and insulin sensitivity in mice lacking the isocitrate dehydrogenase 2 gene. *Free Radic. Biol. Med.* **2016**, *99*, 179–188. [[CrossRef](#)] [[PubMed](#)]
25. Liu, Y.; Li, Y.; Liang, J.; Sun, Z.; Wu, Q.; Liu, Y.; Sun, C. The Mechanism of Leptin on Inhibiting Fibrosis and Promoting Browning of White Fat by Reducing ITGA5 in Mice. *Int. J. Mol. Sci.* **2021**, *22*, 2353. [[CrossRef](#)] [[PubMed](#)]
26. Morandi, E.M.; Verstappen, R.; Zwierzina, M.E.; Geley, S.; Pierer, G.; Ploner, C. ITGAV and ITGA5 diversely regulate proliferation and adipogenic differentiation of human adipose derived stem cells. *Sci. Rep.* **2016**, *6*, 28889. [[CrossRef](#)] [[PubMed](#)]
27. Jelinek, D.; Heidenreich, R.A.; Erickson, R.P.; Garver, W.S. Decreased Npc1 gene dosage in mice is associated with weight gain. *Obesity* **2010**, *18*, 1457–1459. [[CrossRef](#)]
28. Liu, R.; Zou, Y.; Hong, J.; Cao, M.; Cui, B.; Zhang, H.; Chen, M.; Shi, J.; Ning, T.; Zhao, S.; et al. Rare Loss-of-Function Variants in NPC1 Predispose to Human Obesity. *Diabetes* **2017**, *66*, 935–947. [[CrossRef](#)]
29. Jelinek, D.; Millward, V.; Birdi, A.; Trouard, T.P.; Heidenreich, R.A.; Garver, W.S. Npc1 haploinsufficiency promotes weight gain and metabolic features associated with insulin resistance. *Hum. Mol. Genet.* **2011**, *20*, 312–321. [[CrossRef](#)]
30. Castillo, J.J.; Jelinek, D.; Wei, H.; Gannon, N.P.; Vaughan, R.A.; Horwood, L.J.; Meaney, F.J.; Garcia-Smith, R.; Trujillo, K.A.; Heidenreich, R.A.; et al. The Niemann-Pick C1 gene interacts with a high-fat diet to promote weight gain through differential regulation of central energy metabolism pathways. *Am. J. Physiol. Endocrinol. Metab.* **2017**, *313*, E183–E194. [[CrossRef](#)]
31. Bambace, C.; Dahlman, I.; Arner, P.; Kulyté, A. NPC1 in human white adipose tissue and obesity. *BMC Endocr. Disord.* **2013**, *13*, 5. [[CrossRef](#)] [[PubMed](#)]
32. Bernhard, F.; Landgraf, K.; Klötting, N.; Berthold, A.; Büttner, P.; Friebe, D.; Kiess, W.; Kovacs, P.; Blüher, M.; Körner, A. Functional relevance of genes implicated by obesity genome-wide association study signals for human adipocyte biology. *Diabetologia* **2013**, *56*, 311–322. [[CrossRef](#)] [[PubMed](#)]
33. Moreno, M.; Ortega, F.; Xifra, G.; Ricart, W.; Fernández-Real, J.M.; Moreno-Navarrete, J.M. Cytosolic aconitase activity sustains adipogenic capacity of adipose tissue connecting iron metabolism and adipogenesis. *FASEB J. Off. Publ. Fed. Am. Soc. Exp. Biol.* **2015**, *29*, 1529–1539. [[CrossRef](#)] [[PubMed](#)]
34. Masson, O.; Chavey, C.; Dray, C.; Meulle, A.; Daviaud, D.; Quilliot, D.; Muller, C.; Valet, P.; Liaudet-Coopman, E. LRP1 receptor controls adipogenesis and is up-regulated in human and mouse obese adipose tissue. *PLoS ONE* **2009**, *4*, e7422. [[CrossRef](#)] [[PubMed](#)]
35. Woldt, E.; Matz, R.L.; Terrand, J.; Mlih, M.; Gracia, C.; Foppolo, S.; Martin, S.; Bruban, V.; Ji, J.; Velot, E.; et al. Differential signaling by adaptor molecules LRP1 and ShcA regulates adipogenesis by the insulin-like growth factor-1 receptor. *J. Biol. Chem.* **2011**, *286*, 16775–16782. [[CrossRef](#)]
36. Qu, J.; Fourman, S.; Fitzgerald, M.; Liu, M.; Nair, S.; Osés-Prieto, J.; Burlingame, A.; Morris, J.H.; Davidson, W.S.; Tso, P.; et al. Low-density lipoprotein receptor-related protein 1 (LRP1) is a novel receptor for apolipoprotein A4 (APOA4) in adipose tissue. *Sci. Rep.* **2021**, *11*, 13289. [[CrossRef](#)]
37. Shin, S.; Seong, J.K.; Bae, Y.S. Ahnak stimulates BMP2-mediated adipocyte differentiation through Smad1 activation. *Obesity* **2016**, *24*, 398–407. [[CrossRef](#)]

38. Shin, J.H.; Kim, I.Y.; Kim, Y.N.; Shin, S.M.; Roh, K.J.; Lee, S.H.; Sohn, M.; Cho, S.Y.; Lee, S.H.; Ko, C.-Y.; et al. Obesity Resistance and Enhanced Insulin Sensitivity in Ahnak^{-/-} Mice Fed a High Fat Diet Are Related to Impaired Adipogenesis and Increased Energy Expenditure. *PLoS ONE* **2015**, *10*, e0139720. [[CrossRef](#)]
39. Woo, J.K.; Shin, J.H.; Lee, S.H.; Park, H.-M.; Cho, S.Y.; Sung, Y.M.; Kim, I.Y.; Seong, J.K. Essential role of Ahnak in adipocyte differentiation leading to the transcriptional regulation of Bmpr1 α expression. *Cell Death Dis.* **2018**, *9*, 864. [[CrossRef](#)]
40. Yang, W.; Thein, S.; Lim, C.-Y.; Ericksen, R.E.; Sugii, S.; Xu, F.; Robinson, R.C.; Kim, J.B.; Han, W. Arp2/3 complex regulates adipogenesis by controlling cortical actin remodelling. *Biochem. J.* **2014**, *464*, 179–192. [[CrossRef](#)]
41. Kerr, A.G.; Sinha, I.; Dadvar, S.; Arner, P.; Dahlman, I. Epigenetic regulation of diabetogenic adipose morphology. *Mol. Metab.* **2019**, *25*, 159–167. [[CrossRef](#)] [[PubMed](#)]
42. Morales, L.D.; Cromack, D.T.; Tripathy, D.; Fourcaudot, M.; Kumar, S.; Curran, J.E.; Carless, M.; Göring, H.H.H.; Hu, S.L.; Lopez-Alvarenga, J.C.; et al. Further evidence supporting a potential role for ADH1B in obesity. *Sci. Rep.* **2021**, *11*, 1932. [[CrossRef](#)] [[PubMed](#)]
43. Haenisch, M.; Nguyen, T.; Fihn, C.A.; Goldstein, A.S.; Amory, J.K.; Treuting, P.; Brabb, T.; Paik, J. Investigation of an ALDH1A1-specific inhibitor for suppression of weight gain in a diet-induced mouse model of obesity. *Int. J. Obes.* **2021**, *45*, 1542–1552. [[CrossRef](#)] [[PubMed](#)]
44. Reichert, B.; Yasmeen, R.; Jeyakumar, S.M.; Yang, F.; Thomou, T.; Alder, H.; Duyster, G.; Maiseyeu, A.; Mihai, G.; Harrison, E.H.; et al. Concerted action of aldehyde dehydrogenases influences depot-specific fat formation. *Mol. Endocrinol.* **2011**, *25*, 799–809. [[CrossRef](#)] [[PubMed](#)]
45. Wang, P.; Mariman, E.; Keijer, J.; Bouwman, F.; Noben, J.-P.; Robben, J.; Renes, J. Profiling of the secreted proteins during 3T3-L1 adipocyte differentiation leads to the identification of novel adipokines. *Cell. Mol. Life Sci.* **2004**, *61*, 2405–2417. [[CrossRef](#)] [[PubMed](#)]
46. Baek, J.-H.; Kim, D.-H.; Lee, J.; Kim, S.-J.; Chun, K.-H. Galectin-1 accelerates high-fat diet-induced obesity by activation of peroxisome proliferator-activated receptor gamma (PPAR γ) in mice. *Cell Death Dis.* **2021**, *12*, 66. [[CrossRef](#)] [[PubMed](#)]
47. Roumans, N.J.T.; Vink, R.G.; Bouwman, F.G.; Fazelzadeh, P.; van Baak, M.A.; Mariman, E.C.M. Weight loss-induced cellular stress in subcutaneous adipose tissue and the risk for weight regain in overweight and obese adults. *Int. J. Obes.* **2017**, *41*, 894–901. [[CrossRef](#)]
48. Mukherjee, R.; Yun, J.W. Pharmacological inhibition of galectin-1 by lactulose alleviates weight gain in diet-induced obese rats. *Life Sci.* **2016**, *148*, 112–117. [[CrossRef](#)]
49. Mukherjee, R.; Kim, S.W.; Park, T.; Choi, M.S.; Yun, J.W. Targeted inhibition of galectin 1 by thiodigalactoside dramatically reduces body weight gain in diet-induced obese rats. *Int. J. Obes.* **2015**, *39*, 1349–1358. [[CrossRef](#)]
50. Fryk, E.; Strindberg, L.; Lundqvist, A.; Sandstedt, M.; Bergfeldt, L.; Mattsson Hultén, L.; Bergström, G.; Jansson, P.-A. Galectin-1 is inversely associated with type 2 diabetes independently of obesity—A SCAPIS pilot study. *Metab. Open* **2019**, *4*, 100017. [[CrossRef](#)]
51. Acar, S.; Paketçi, A.; Küme, T.; Tuhan, H.; Gürsoy Çalan, Ö.; Demir, K.; Böber, E.; Abaci, A. Serum galectin-1 levels are positively correlated with body fat and negatively with fasting glucose in obese children. *Peptides* **2017**, *95*, 51–56. [[CrossRef](#)] [[PubMed](#)]
52. Ande, S.R.; Xu, Z.; Gu, Y.; Mishra, S. Prohibitin has an important role in adipocyte differentiation. *Int. J. Obes.* **2012**, *36*, 1236–1244. [[CrossRef](#)] [[PubMed](#)]
53. Liu, D.; Lin, Y.; Kang, T.; Huang, B.; Xu, W.; Garcia-Barrio, M.; Olatinwo, M.; Matthews, R.; Chen, Y.E.; Thompson, W.E. Mitochondrial dysfunction and adipogenic reduction by prohibitin silencing in 3T3-L1 cells. *PLoS ONE* **2012**, *7*, e34315. [[CrossRef](#)] [[PubMed](#)]
54. Kang, T.; Lu, W.; Xu, W.; Anderson, L.; Bacanamwo, M.; Thompson, W.; Chen, Y.E.; Liu, D. MicroRNA-27 (miR-27) targets prohibitin and impairs adipocyte differentiation and mitochondrial function in human adipose-derived stem cells. *J. Biol. Chem.* **2013**, *288*, 34394–34402. [[CrossRef](#)]
55. Salameh, A.; Daquinag, A.C.; Staquicini, D.I.; An, Z.; Hajjar, K.A.; Pasqualini, R.; Arap, W.; Kolonin, M.G. Prohibitin/annexin 2 interaction regulates fatty acid transport in adipose tissue. *JCI Insight* **2016**, *1*, e86351. [[CrossRef](#)]
56. Gesta, S.; Guntur, K.; Majumdar, I.D.; Akella, S.; Vishnudas, V.K.; Sarangarajan, R.; Narain, N.R. Reduced expression of collagen VI alpha 3 (COL6A3) confers resistance to inflammation-induced MCP1 expression in adipocytes. *Obesity* **2016**, *24*, 1695–1703. [[CrossRef](#)]
57. Pardo, F.; Villalobos-Labra, R.; Sobrevia, B.; Toledo, F.; Sobrevia, L. Extracellular vesicles in obesity and diabetes mellitus. *Mol. Aspects Med.* **2018**, *60*, 81–91. [[CrossRef](#)]
58. Dankel, S.N.; Svärd, J.; Matthä, S.; Claussnitzer, M.; Klötting, N.; Glunk, V.; Fandalyuk, Z.; Grytten, E.; Solsvik, M.H.; Nielsen, H.-J.; et al. COL6A3 expression in adipocytes associates with insulin resistance and depends on PPAR γ and adipocyte size. *Obesity* **2014**, *22*, 1807–1813. [[CrossRef](#)]
59. Pasarica, M.; Gowronska-Kozak, B.; Burk, D.; Remedios, I.; Hymel, D.; Gimble, J.; Ravussin, E.; Bray, G.A.; Smith, S.R. Adipose tissue collagen VI in obesity. *J. Clin. Endocrinol. Metab.* **2009**, *94*, 5155–5162. [[CrossRef](#)]
60. Kosicka, A.; Cunliffe, A.D.; Mackenzie, R.; Zariwala, M.G.; Perretti, M.; Flower, R.J.; Renshaw, D. Attenuation of plasma annexin A1 in human obesity. *FASEB J. Off. Publ. Fed. Am. Soc. Exp. Biol.* **2013**, *27*, 368–378. [[CrossRef](#)]

61. Warne, J.P.; John, C.D.; Christian, H.C.; Morris, J.F.; Flower, R.J.; Sugden, D.; Solito, E.; Gillies, G.E.; Buckingham, J.C. Gene deletion reveals roles for annexin A1 in the regulation of lipolysis and IL-6 release in epididymal adipose tissue. *Am. J. Physiol. Endocrinol. Metab.* **2006**, *291*, E1264–E1273. [[CrossRef](#)] [[PubMed](#)]
62. Hogarth, M.W.; Defour, A.; Lazarski, C.; Gallardo, E.; Diaz Manera, J.; Partridge, T.A.; Nagaraju, K.; Jaiswal, J.K. Fibroadipogenic progenitors are responsible for muscle loss in limb girdle muscular dystrophy 2B. *Nat. Commun.* **2019**, *10*, 2430. [[CrossRef](#)] [[PubMed](#)]
63. Ji, L.; Zhao, Y.; He, L.; Zhao, J.; Gao, T.; Liu, F.; Qi, B.; Kang, F.; Wang, G.; Zhao, Y.; et al. AKAP1 Deficiency Attenuates Diet-Induced Obesity and Insulin Resistance by Promoting Fatty Acid Oxidation and Thermogenesis in Brown Adipocytes. *Adv. Sci.* **2021**, *8*, 2002794. [[CrossRef](#)] [[PubMed](#)]
64. Joseph, R.; Poschmann, J.; Sukarieh, R.; Too, P.G.; Julien, S.G.; Xu, F.; Teh, A.L.; Holbrook, J.D.; Ng, K.L.; Chong, Y.S.; et al. ACSL1 Is Associated With Fetal Programming of Insulin Sensitivity and Cellular Lipid Content. *Mol. Endocrinol.* **2015**, *29*, 909–920. [[CrossRef](#)]
65. Ellis, J.M.; Li, L.O.; Wu, P.-C.; Koves, T.R.; Ilkayeva, O.; Stevens, R.D.; Watkins, S.M.; Muoio, D.M.; Coleman, R.A. Adipose acyl-CoA synthetase-1 directs fatty acids toward beta-oxidation and is required for cold thermogenesis. *Cell Metab.* **2010**, *12*, 53–64. [[CrossRef](#)]
66. Lobo, S.; Wiczler, B.M.; Bernlohr, D.A. Functional analysis of long-chain acyl-CoA synthetase 1 in 3T3-L1 adipocytes. *J. Biol. Chem.* **2009**, *284*, 18347–18356. [[CrossRef](#)]
67. Liu, Q.; Gauthier, M.-S.; Sun, L.; Ruderman, N.; Lodish, H. Activation of AMP-activated protein kinase signaling pathway by adiponectin and insulin in mouse adipocytes: Requirement of acyl-CoA synthetases FATP1 and Acsl1 and association with an elevation in AMP/ATP ratio. *FASEB J. Off. Publ. Fed. Am. Soc. Exp. Biol.* **2010**, *24*, 4229–4239. [[CrossRef](#)]
68. Yi, X.; Liu, J.; Wu, P.; Gong, Y.; Xu, X.; Li, W. The key microRNA on lipid droplet formation during adipogenesis from human mesenchymal stem cells. *J. Cell. Physiol.* **2020**, *235*, 328–338. [[CrossRef](#)]
69. Zhan, T.; Poppelreuther, M.; Eehalt, R.; Füllekrug, J. Overexpressed FATP1, ACSVL4/FATP4 and ACSL1 increase the cellular fatty acid uptake of 3T3-L1 adipocytes but are localized on intracellular membranes. *PLoS ONE* **2012**, *7*, e45087. [[CrossRef](#)]
70. Richards, M.R.; Harp, J.D.; Ory, D.S.; Schaffer, J.E. Fatty acid transport protein 1 and long-chain acyl coenzyme A synthetase 1 interact in adipocytes. *J. Lipid Res.* **2006**, *47*, 665–672. [[CrossRef](#)]
71. Siang, D.T.C.; Lim, Y.C.; Kyaw, A.M.M.; Win, K.N.; Chia, S.Y.; Degirmenci, U.; Hu, X.; Tan, B.C.; Walet, A.C.E.; Sun, L.; et al. The RNA-binding protein HuR is a negative regulator in adipogenesis. *Nat. Commun.* **2020**, *11*, 213. [[CrossRef](#)] [[PubMed](#)]
72. Li, J.; Gong, L.; Liu, S.; Zhang, Y.; Zhang, C.; Tian, M.; Lu, H.; Bu, P.; Yang, J.; Ouyang, C.; et al. Adipose HuR protects against diet-induced obesity and insulin resistance. *Nat. Commun.* **2019**, *10*, 2375. [[CrossRef](#)] [[PubMed](#)]
73. Gantt, K.; Cherry, J.; Tenney, R.; Karschner, V.; Pekala, P.H. An early event in adipogenesis, the nuclear selection of the CCAAT enhancer-binding protein {beta} (C/EBP{beta}) mRNA by HuR and its translocation to the cytosol. *J. Biol. Chem.* **2005**, *280*, 24768–24774. [[CrossRef](#)] [[PubMed](#)]
74. Karschner, V.A.; Pekala, P.H. HuR involvement in mitotic clonal expansion during acquisition of the adipocyte phenotype. *Biochem. Biophys. Res. Commun.* **2009**, *383*, 203–205. [[CrossRef](#)]
75. Bibli, S.-I.; Hu, J.; Sigala, F.; Wittig, I.; Heidler, J.; Zukunft, S.; Tsilimigras, D.I.; Randriamboavonjy, V.; Wittig, J.; Kojonazarov, B.; et al. Cystathionine γ Lyase Sulfhydrates the RNA Binding Protein Human Antigen R to Preserve Endothelial Cell Function and Delay Atherogenesis. *Circulation* **2019**, *139*, 101–114. [[CrossRef](#)]
76. Ding, Y.; Wang, H.; Geng, B.; Xu, G. Sulfhydrylation of perilipin 1 is involved in the inhibitory effects of cystathionine gamma lyase/hydrogen sulfide on adipocyte lipolysis. *Biochem. Biophys. Res. Commun.* **2020**, *521*, 786–790. [[CrossRef](#)]
77. Kaminska, D.; Hämäläinen, M.; Cederberg, H.; Käkälä, P.; Venesmaa, S.; Miettinen, P.; Ilves, I.; Herzig, K.-H.; Kolehmainen, M.; Karhunen, L.; et al. Adipose tissue INSR splicing in humans associates with fasting insulin level and is regulated by weight loss. *Diabetologia* **2014**, *57*, 347–351. [[CrossRef](#)]
78. Stadion, M.; Schwerbel, K.; Graja, A.; Baumeier, C.; Rödigier, M.; Jonas, W.; Wolfrum, C.; Staiger, H.; Fritsche, A.; Häring, H.-U.; et al. Increased Ifi202b/IFI16 expression stimulates adipogenesis in mice and humans. *Diabetologia* **2018**, *61*, 1167–1179. [[CrossRef](#)]
79. Valentino, R.; D’Esposito, V.; Passaretti, F.; Liotti, A.; Cabaro, S.; Longo, M.; Perruolo, G.; Oriente, F.; Beguinot, F.; Formisano, P. Bisphenol-A impairs insulin action and up-regulates inflammatory pathways in human subcutaneous adipocytes and 3T3-L1 cells. *PLoS ONE* **2013**, *8*, e82099. [[CrossRef](#)]
80. Guo, T.; Gupta, A.; Yu, J.; Granados, J.Z.; Gandhi, A.Y.; Evers, B.M.; Iyengar, P.; Infante, R.E. LIFR- α -dependent adipocyte signaling in obesity limits adipose expansion contributing to fatty liver disease. *iScience* **2021**, *24*, 102227. [[CrossRef](#)]
81. Berg, A.H.; Lin, Y.; Lisanti, M.P.; Scherer, P.E. Adipocyte differentiation induces dynamic changes in NF-kappaB expression and activity. *Am. J. Physiol. Endocrinol. Metab.* **2004**, *287*, E1178–E1188. [[CrossRef](#)] [[PubMed](#)]
82. Tang, T.; Zhang, J.; Yin, J.; Staszkiwicz, J.; Gawronska-Kozak, B.; Jung, D.Y.; Ko, H.J.; Ong, H.; Kim, J.K.; Mynatt, R.; et al. Uncoupling of inflammation and insulin resistance by NF-kappaB in transgenic mice through elevated energy expenditure. *J. Biol. Chem.* **2010**, *285*, 4637–4644. [[CrossRef](#)] [[PubMed](#)]
83. Lee, K.; Um, S.H.; Rhee, D.K.; Pyo, S. Interferon-alpha inhibits adipogenesis via regulation of JAK/STAT1 signaling. *Biochim. Biophys. Acta* **2016**, *1860*, 2416–2427. [[CrossRef](#)] [[PubMed](#)]
84. Chernis, N.; Masschelin, P.; Cox, A.R.; Hartig, S.M. Bisphenol AF promotes inflammation in human white adipocytes. *Am. J. Physiol. Cell Physiol.* **2020**, *318*, C63–C72. [[CrossRef](#)] [[PubMed](#)]

85. Annamalai, D.; Clipstone, N.A. Prostaglandin F₂ α inhibits adipogenesis via an autocrine-mediated interleukin-11/glycoprotein 130/STAT1-dependent signaling cascade. *J. Cell. Biochem.* **2014**, *115*, 1308–1321. [[CrossRef](#)]
86. Antony, A.; Lian, Z.; Perrard, X.D.; Perrard, J.; Liu, H.; Cox, A.R.; Saha, P.; Hennighausen, L.; Hartig, S.M.; Ballantyne, C.M.; et al. Deficiency of Stat1 in CD11c(+) Cells Alters Adipose Tissue Inflammation and Improves Metabolic Dysfunctions in Mice Fed a High-Fat Diet. *Diabetes* **2021**, *70*, 720–732. [[CrossRef](#)]
87. Chattopadhyay, D.; Das, S.; Guria, S.; Basu, S.; Mukherjee, S. Fetuin-A regulates adipose tissue macrophage content and activation in insulin resistant mice through MCP-1 and iNOS: Involvement of IFN γ -JAK2-STAT1 pathway. *Biochem. J.* **2021**, *478*, 4027–4043. [[CrossRef](#)]
88. Cox, A.R.; Chernis, N.; Bader, D.A.; Saha, P.K.; Masschelin, P.M.; Felix, J.B.; Sharp, R.; Lian, Z.; Putluri, V.; Rajapakshe, K.; et al. STAT1 Dissociates Adipose Tissue Inflammation From Insulin Sensitivity in Obesity. *Diabetes* **2020**, *69*, 2630–2641. [[CrossRef](#)]
89. Isakson, P.; Hammarstedt, A.; Gustafson, B.; Smith, U. Impaired preadipocyte differentiation in human abdominal obesity: Role of Wnt, tumor necrosis factor-alpha, and inflammation. *Diabetes* **2009**, *58*, 1550–1557. [[CrossRef](#)]
90. Tang, X.; Guilherme, A.; Chakladar, A.; Powelka, A.M.; Konda, S.; Virbasius, J.V.; Nicoloso, S.M.C.; Straubhaar, J.; Czech, M.P. An RNA interference-based screen identifies MAP4K4/NIK as a negative regulator of PPAR γ , adipogenesis, and insulin-responsive hexose transport. *Proc. Natl. Acad. Sci. USA* **2006**, *103*, 2087–2092. [[CrossRef](#)]
91. Danai, L.V.; Guilherme, A.; Guntur, K.V.; Straubhaar, J.; Nicoloso, S.M.; Czech, M.P. Map4k4 suppresses Srebp-1 and adipocyte lipogenesis independent of JNK signaling. *J. Lipid Res.* **2013**, *54*, 2697–2707. [[CrossRef](#)] [[PubMed](#)]
92. Danai, L.V.; Flach, R.J.R.; Virbasius, J.V.; Menendez, L.G.; Jung, D.Y.; Kim, J.H.; Kim, J.K.; Czech, M.P. Inducible Deletion of Protein Kinase Map4k4 in Obese Mice Improves Insulin Sensitivity in Liver and Adipose Tissues. *Mol. Cell. Biol.* **2015**, *35*, 2356–2365. [[CrossRef](#)] [[PubMed](#)]
93. Li, J.; Muraio, K.; Imachi, H.; Yu, X.; Muraoka, T.; Kim, J.B.; Ishida, T. Prolactin regulatory element-binding protein involved in cAMP-mediated suppression of adiponectin gene. *J. Cell. Mol. Med.* **2010**, *14*, 1294–1302. [[CrossRef](#)] [[PubMed](#)]
94. Wang, S.; Crisman, L.; Miller, J.; Datta, I.; Gulbranson, D.R.; Tian, Y.; Yin, Q.; Yu, H.; Shen, J. Inducible Exoc7/Exo70 knockout reveals a critical role of the exocyst in insulin-regulated GLUT4 exocytosis. *J. Biol. Chem.* **2019**, *294*, 19988–19996. [[CrossRef](#)]
95. Lizunov, V.A.; Lisinski, I.; Stenkula, K.; Zimmerberg, J.; Cushman, S.W. Insulin regulates fusion of GLUT4 vesicles independent of Exo70-mediated tethering. *J. Biol. Chem.* **2009**, *284*, 7914–7919. [[CrossRef](#)]
96. Tominaga, K.; Kagata, T.; Johmura, Y.; Hishida, T.; Nishizuka, M.; Imagawa, M. SLC39A14, a LZT protein, is induced in adipogenesis and transports zinc. *FEBS J.* **2005**, *272*, 1590–1599. [[CrossRef](#)]
97. Troche, C.; Aydemir, T.B.; Cousins, R.J. Zinc transporter Slc39a14 regulates inflammatory signaling associated with hypertrophic adiposity. *Am. J. Physiol. Endocrinol. Metab.* **2016**, *310*, E258–E268. [[CrossRef](#)]
98. Fu, L.; Liu, K.; He, J.; Tian, C.; Yu, X.; Yang, J. Direct Proteomic Mapping of Cysteine Persulfidation. *Antioxid. Redox Signal.* **2020**, *33*, 1061–1076. [[CrossRef](#)]
99. Wang, Z.; Dou, X.; Yao, T.; Song, Z. Homocysteine inhibits adipogenesis in 3T3-L1 preadipocytes. *Exp. Biol. Med.* **2011**, *236*, 1379–1388. [[CrossRef](#)]
100. Steinbrenner, H.; Micoogullari, M.; Hoang, N.A.; Bergheim, I.; Klotz, L.-O.; Sies, H. Selenium-binding protein 1 (SELENBP1) is a marker of mature adipocytes. *Redox Biol.* **2019**, *20*, 489–495. [[CrossRef](#)]
101. Randi, E.B.; Casili, G.; Jacquemai, S.; Szabo, C. Selenium-Binding Protein 1 (SELENBP1) Supports Hydrogen Sulfide Biosynthesis and Adipogenesis. *Antioxidants* **2021**, *10*, 361. [[CrossRef](#)] [[PubMed](#)]
102. Yang, J.; Minkler, P.; Grove, D.; Wang, R.; Willard, B.; Dweik, R.; Hine, C. Non-enzymatic hydrogen sulfide production from cysteine in blood is catalyzed by iron and vitamin B₆. *Commun. Biol.* **2019**, *2*, 88–97. [[CrossRef](#)] [[PubMed](#)]